

THE CRYSTAL CHEMISTRY, STRUCTURE AND PROPERTIES OF A SYNTHETIC CARNOTITE-TYPE COMPOUND, $\text{Ba}_2[(\text{UO}_2)_2\text{Ti}_2\text{O}_8]$

KIA S. WALLWORK[§] AND MICHAEL JAMES

Bragg Institute, ANSTO, PMB 1, Menai, New South Wales 2234, Australia

MELODY L. CARTER

Materials and Engineering Science Division, ANSTO, PMB 1, Menai, New South Wales 2234, Australia

ABSTRACT

The crystal structure of the carnotite-type compound $\text{Ba}_2[(\text{UO}_2)_2\text{Ti}_2\text{O}_8]$ has been determined by *ab initio* methods from synchrotron X-ray and neutron powder-diffraction data. We describe the first reported structure of a uranyl titanate; it was solved in the monoclinic space-group $P2_1/c$ and has the lattice parameters a 6.4463(1), b 8.5999(1), c 10.2532(1) Å, β 75.936(1)°, V 551.36(1) Å³, D_{calc} 6.253 g/cm³ and $Z = 4$. A multiple histogram approach was used to refine the structure from synchrotron and neutron-diffraction data, giving quality factors of R_B 0.032 and 0.039, R_{wp} 0.090 and 0.063, and R_p 0.070 and 0.049, respectively. The compound forms a layered structure in which sheets of uranyl pentagonal bipyramids share edges with dimers of TiO_5 square pyramids. These are separated by layers of 11-fold-coordinated barium atoms. Because of the potential presence of $\text{Ba}_2[(\text{UO}_2)_2\text{Ti}_2\text{O}_8]$ in ceramic waste-forms for the immobilization of radioactive wastes, the leach rate of uranium and barium were determined. The normalized rates of leaching from $\text{Ba}_2[(\text{UO}_2)_2\text{Ti}_2\text{O}_8]$, averaged over seven days, are 1.3×10^{-5} g/m²/day for uranium, a significantly lower rate than that observed from pyrochlore waste-forms, and 1×10^{-4} g/m²/day for barium.

Keywords: $\text{Ba}_2[(\text{UO}_2)_2\text{Ti}_2\text{O}_8]$, crystal structure, uranyl titanate waste-form, synchrotron data, neutron-diffraction data, powder diffraction.

SOMMAIRE

Nous avons déterminé la structure cristalline d'un composé de type carnotite, $\text{Ba}_2[(\text{UO}_2)_2\text{Ti}_2\text{O}_8]$, par méthodes *ab initio* à partir de données de diffraction X (rayonnement synchrotron) et diffraction de neutrons. Nous décrivons pour la première fois la structure d'un titanate uranylé; elle a été résolue dans le groupe spatial $P2_1/c$, système monoclinique, avec les paramètres réticulaires a 6.4463(1), b 8.5999(1), c 10.2532(1) Å, β 75.936(1)°, V 551.36(1) Å³, D_{calc} 6.253 g/cm³ et $Z = 4$. Des histogrammes multiples ont été utilisés pour affiner la structure à partir des données obtenues avec rayonnement synchrotron et diffraction de neutrons, ce qui a donné les valeurs suivantes des indices de qualité: R_B 0.032 et 0.039, R_{wp} 0.090 et 0.063, et R_p 0.070 et 0.049, respectivement. Le composé a une structure en couches, dans lesquelles les bipyramides uranylées pentagonales partagent des arêtes avec les pyramides carrées TiO_5 . Ces feuillettes sont séparés par des feuillettes d'atomes de barium à coordinence 11. Vue la possibilité d'utiliser le composé $\text{Ba}_2[(\text{UO}_2)_2\text{Ti}_2\text{O}_8]$ comme matériau céramique pour l'immobilisation de déchets radioactifs, nous avons déterminé le taux de lessivage de l'uranium et du barium. Les taux de lessivage du composé $\text{Ba}_2[(\text{UO}_2)_2\text{Ti}_2\text{O}_8]$, normalisés sur sept jours, sont 1.3×10^{-5} g/m²/jour pour l'uranium, ce qui est sensiblement plus faible que les taux observés avec un matériau à structure de pyrochlore, et 1×10^{-4} g/m²/jour pour le barium.

(Traduit par la Rédaction)

Mots-clés: $\text{Ba}_2[(\text{UO}_2)_2\text{Ti}_2\text{O}_8]$, structure cristalline, titanate uranylé pour l'enfouissement des déchets, données de synchrotron, données de diffraction de neutrons, diffraction sur poudre.

[§] Current address: Australian Synchrotron, 800 Blackburn Road, Clayton, Victoria 3168, Australia.
E-mail address: kia.wallwork@synchrotron.vic.gov.au

INTRODUCTION

The immobilization of High-Level radioactive Wastes (HLW) in stable matrices for long-term storage, or geological disposal, is an important step in the closed nuclear fuel cycle. In 1979, Ringwood *et al.* suggested that assemblages of titanate minerals could be used to incorporate HLW because titanate minerals are much more water-resistant than those used in supercalcline (McCarthy 1977), which was the principal alternative to borosilicate glass at that time. Synthetic titanate compounds such as brannerite, UTi_2O_6 (Szymański & Scott 1982, James & Watson 2002) and a uranium-containing pyrochlore-group phase, CaUTi_2O_7 (Dickson *et al.* 1989) have the capacity to take up all the elements in HLW into their crystal structures at regular lattice-sites in the form of solid solutions. In recent years, titanate ceramics containing 80–90 vol.% pyrochlore-type material, for example $(\text{Ca,REE,Ac})_2\text{Ti}_2\text{O}_7$ (where REE represents rare-earth elements and Ac represents the actinides) have been considered to be promising matrices for the immobilization of wastes with high actinide content, particularly excess weapons plutonium (Vance *et al.* 1997, Ebbinghaus *et al.* 1998). In a recent study of the phase development of pyrochlore-brannerite-based ceramics and their possible methods of consolidation, Stefanovsky *et al.* (2001) reported the phase BaUTi_2O_7 in a titanate ceramic consolidated by melting. More recently, Vance *et al.* (2002) examined materials synthesized with nominal compositions BaUTiO_5 and BaUTi_2O_7 , which were either sintered or melted in air or argon. In each case, scanning electron microscopy with energy-dispersion spectrometry (EDS) suggested BaUTiO_x (x in the range 5–6) and not BaUTi_2O_7 to be the more likely product. They characterized the valence state of U in these materials by X-ray absorption spectroscopy and found the U to be hexavalent in all samples, thus making $x = 6$. Whereas the combination of these studies revealed that BaUTiO_6 does not adopt the pyrochlore structure, they did not lead to the possible assignment of a crystal structure for this phase.

We report here the structural solution of $\text{Ba}_2[(\text{UO}_2)_2\text{Ti}_2\text{O}_8]$ prepared by sintering in argon, as investigated by synchrotron X-ray and neutron powder-diffraction methods. Leach testing was also carried out to determine whether the presence of $\text{Ba}_2[(\text{UO}_2)_2\text{Ti}_2\text{O}_8]$ in ceramic waste-forms would be detrimental to the durability of pyrochlore- or brannerite-type wastes.

EXPERIMENTAL METHODS

Synthesis

A sample with the nominal composition BaUTiO_6 (20 g) was prepared by the alkoxide route (Ringwood *et al.* 1988). This method involves mixing titanium (Ti^{4+})

isopropoxide (12.93 g) in ethanol (50 mL). Barium nitrate (11.9 g) and uranium nitrate (22.86 g) were dissolved in 100 mL of water heated to $\sim 90^\circ\text{C}$. The two solutions are then mixed together in a stainless steel beaker using a shear mixer (at 1000 rpm). The mixture was then heated in the stainless steel beaker in an oven at $\sim 110^\circ\text{C}$ to dryness. The dry product was transferred to an alumina crucible and calcined in air for two hours at 750°C . The product (20 g added to ~ 70 mL water) was then wet-ball-milled using Y-stabilized ZrO_2 10-mm balls in a 200 mL (~ 70 mm diameter) ball mill rotating at ~ 75 rpm for 16 hours. Ten grams of the sample was pressed in a steel die 20 mm in diameter under a pressure of 50 MPa. The pellets were placed on Pt foil and sintered in flowing argon (99.999% purity) for 16 hours at 1400°C . Prior to X-ray diffraction, the samples were ground by hand using an agate mortar and pestle.

Scanning electron microscopy

The products of synthesis were examined by scanning electron microscopy (SEM) using a JEOL JSM6400 scanning electron microscope, equipped with a Noran Voyager Series IV energy-dispersion spectroscopy (EDS) system operated at 15 keV.

Powder X-ray diffraction

Powder X-ray-diffraction measurements were made on a Scintag Inc. XGEN 4000 X-ray diffractometer at ambient temperature using $\text{CuK}\alpha$ radiation. Diffraction samples were prepared by crushing the sintered $\text{Ba}_2[(\text{UO}_2)_2\text{Ti}_2\text{O}_8]$ to a fine powder and side-loading it into the sample holder. Data were collected over the angular range $5^\circ \leq 2\theta \leq 80^\circ$ ($17.659 \text{ \AA} \geq d \geq 1.198 \text{ \AA}$), in 0.05° steps, with counting times of 10 s per step.

Synchrotron X-ray-diffraction analysis of powder

Synchrotron X-ray powder-diffraction data were collected using the ID31 high-resolution powder-diffractometer at the European Synchrotron Research Facility (ESRF). A finely crushed sample was loaded into a glass capillary 0.3 mm in diameter. Data of sufficient quality for structure determination were collected over the angular range $3.5^\circ \leq 2\theta \leq 37.6^\circ$ ($8.188 \text{ \AA} \geq d \geq 0.776 \text{ \AA}$) using a multicrystal analyzer detector in steps of 0.002° . The wavelength of the synchrotron X-rays was $0.5001(1) \text{ \AA}$.

Powder neutron-diffraction analysis

Powder neutron-diffraction data were collected at the Australian Nuclear Science and Technology Organisation's High Flux Australian Reactor (HiFAR) using the high-resolution powder-diffractometer (HRPD). The sample (19.9 g) was loaded into a vanadium sample

cannister 8 mm in diameter. Data were collected for four days at a wavelength of 1.8845(1) Å, over $13^\circ \leq 2\theta \leq 135.7^\circ$; $8.324 \text{ \AA} \geq d \geq 1.017 \text{ \AA}$.

Leach testing

Leach testing was carried out using the Product Consistency Test (PCT-B) (American Society for Testing and Materials 1997). The test was carried out in triplicate at 90°C , over seven days of leaching. The leach-solution concentrations for U and Ba were $1 \times 10^{-4} \text{ g/L}$ and $1 \times 10^{-3} \text{ g/L}$, respectively, and the Ti concentration did not differ significantly from the blank solution.

RESULTS

Scanning electron microscopy of the synthesized compound showed the sample to be largely single-phase $\text{Ba}_2[(\text{UO}_2)_2\text{Ti}_2\text{O}_8]$; very small amounts of UO_2 and BaTiO_3 were found to be present in quantities of less than 0.5%. Secondary electron images of the crushed powder illustrate the plate-like nature of $\text{Ba}_2[(\text{UO}_2)_2\text{Ti}_2\text{O}_8]$ (Fig. 1).

Figure 2 shows the laboratory X-ray-diffraction pattern of $\text{Ba}_2[(\text{UO}_2)_2\text{Ti}_2\text{O}_8]$, collected in Bragg-Brentano geometry. Despite efforts to reduce the preferred orientation of crystallites through side loading, the laboratory diffraction pattern is dominated by only a few lines. Particularly strong peaks were observed at d values of 6.210 Å (I_{rel} 48%), 3.114 Å (I_{rel} 100%) and 2.079 Å (I_{rel} 5%), due to the (100), (200) and (300) reflections, respectively. The background of this pattern

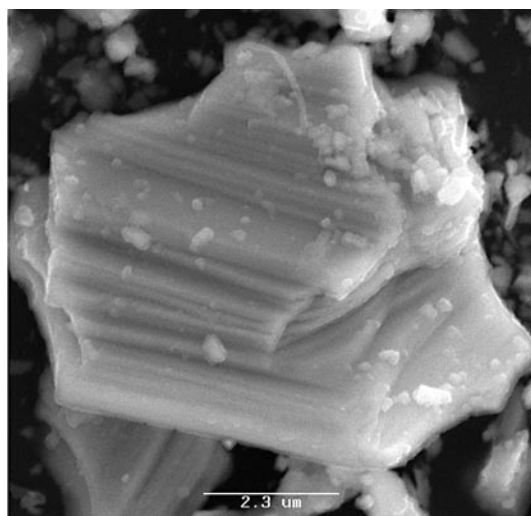


FIG. 1. Scanning electron micrograph of a $\text{Ba}_2[(\text{UO}_2)_2\text{Ti}_2\text{O}_8]$ crystallite showing the platy nature of the crystals.

(Fig. 2 insert) shows many additional weak diffraction lines ($I_{\text{rel}} < 4\%$) also pertaining to this sample. This strong preferred orientation is consistent with the platy morphology of the crystals observed using SEM. The poor signal-to-noise ratio, combined with the low resolution of the diffraction data, precluded indexing of $\text{Ba}_2[(\text{UO}_2)_2\text{Ti}_2\text{O}_8]$ from these data. However, these data can be fit with the unit cell that has since been determined using synchrotron X-ray-diffraction data.

The synchrotron data were used to index the diffraction peaks and to elucidate the structure. By measuring the diffraction pattern of the finely crushed powder in a spinning capillary, the effects of preferred orientation of the crystallites were negated. The very high resolution of the ID31 data (with FWHM of $0.005\text{--}0.039^\circ$ over the data range), allowed the isolation of individual peaks from what is clearly a complex profile and also the determination of a unit cell and space group (as described below).

The X-ray-diffraction data of $\text{Ba}_2[(\text{UO}_2)_2\text{Ti}_2\text{O}_8]$ are dominated by the presence of the heavy atoms U ($Z = 92$) and Ba ($Z = 56$). In comparison, the Ti ($Z = 22$) and O ($Z = 8$) atoms contribute relatively little to the overall scattering. Therefore, additional powder neutron-diffraction data were obtained in order to complete the structure determination and to assist in accurately locating these lighter atoms. The neutron-scattering lengths (b) of uranium, barium, titanium and oxygen are 8.417, 5.07, -3.438 and 5.803 fm ($= 10^{-15} \text{ m}$) respectively (Sears 1992), and indicate that the nuclear scattering is not dominated by the heavy atoms. Again, the cylindrical geometry of the sample, combined with spinning the sample cannister during the neutron-diffraction experiment, allowed these data to be free of preferred orientation effects.

The leach rates of uranium and barium from $\text{Ba}_2[(\text{UO}_2)_2\text{Ti}_2\text{O}_8]$ were determined and normalized

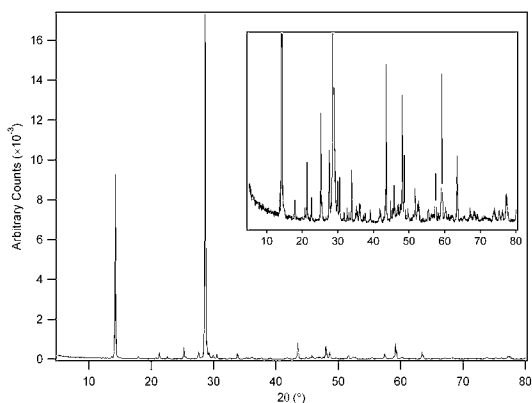


FIG. 2. Observed X-ray powder-diffraction pattern of $\text{Ba}_2[(\text{UO}_2)_2\text{Ti}_2\text{O}_8]$; the insert (on a linear scale) shows an expanded view of the profile.

over the geometric surface-area of the powder (8.5 cm²) in order to directly compare these leach rates with those of synthetic brannerite, UTi₂O₆, and the synthetic U-containing pyrochlore-group phase, CaUTi₂O₇. The leach rate of uranium averaged over seven days from Ba₂[(UO₂)₂Ti₂O₈] is 1.3 × 10⁻⁵ g/m²/day, significantly less than that reported for brannerite (6 × 10⁻² g/m²/day; Zhang *et al.* 2001), and an order of magnitude less than that for U-containing pyrochlore (3 × 10⁻⁴ g/m²/day; Hart *et al.* 1999). The low leach-rate of uranium from Ba₂[(UO₂)₂Ti₂O₈] indicates that the presence of this phase in a waste form would be very beneficial to the durability of the waste form with respect to retention of uranium. This result is in stark contrast to our initial expectations that the presence of Ba₂[(UO₂)₂Ti₂O₈] would degrade the quality of pyrochlore ceramic radioactive waste-forms. The normalized leach-rate for barium is 1 × 10⁻⁴ g/m²/day, two orders of magnitude less than that of Ba from the synthetic hollandite-type phase (Ba,Cs)(Al,Ti)₂Ti₆O₁₆ (Carter *et al.* 2002). Traditionally, hollandite-type titanates are known to effectively immobilize cesium in titanate waste-forms, despite the presence of barium.

The determination of the structure of a "new" phase containing radioactive waste elements is important in the understanding and qualification of a candidate waste-form, and the design of further waste-forms. However, ultimately the durability of the waste-form, when considering its suitability for long-term disposal, is more important than the structure *per se*.

STRUCTURE SOLUTION AND REFINEMENT

The structure analysis was carried out using the RIETICA (Hunter 1998) and SIRPOW.92 (Altomare *et al.* 1994) packages. The powder pattern was indexed using the synchrotron X-ray-diffraction data and the program ITO (Visser 1969), which gave a metrically monoclinic cell. The cell parameters (Table 1) were refined by fitting the whole synchrotron X-ray dataset. The indexed powder pattern indicated that the unit

cell is primitive. Data were extracted from the powder pattern in the form of F_{obs}² values using a Le Bail profile fit within RIETICA. The cell parameters, zero-shift errors and peak-profile parameters were refined simultaneously. A pseudo-Voigt function was used to model the profile shape.

This extraction afforded data for 813 reflections in the form: *hkl*, FWHM, F_{obs}². A search of the reflection data for systematic extinctions did not provide conclusive evidence of the existence of a glide plane, but the presence of a 2₁ axis was expected. With the aid of SIRPOW.92, the motif of the U atom arrangement was established in the space group P2₁/c. The complete structural model was determined by utilizing a modified form of the UO₂(VO₄) sheet found in sengierite, Cu(UO₂)₂(V₂O₈)•6H₂O (Piret *et al.* 1980). The barium atom was initially located on a site equivalent to that of Cu in sengierite. A simultaneous refinement utilizing the synchrotron and neutron-diffraction data was then completed in space group P2₁/c using RIETICA. The profile backgrounds were fitted by Chebyshev type-1 polynomials. In the case of the synchrotron-diffraction data, this function allows the amorphous glass capillary used during data collection to be properly modeled. The X-ray data were corrected for absorption by applying a cylindrical correction of μR = 1.50. The phase scale and the zero shifts were refined, as were all atom coordinates. A single isotropic-displacement parameter was refined for the oxygen atoms, and all non-oxygen displacement parameters were refined individually.

The multiple-histogram structure refinement utilizing the Rietveld method (Rietveld 1969) in RIETICA converged to R_{wp} = 0.090, R_p = 0.070 for the synchrotron refinement and R_{wp} = 0.063, R_p = 0.049 for the neutron refinement. A summary of the data collection, structure solution and refinement is given in Table 1. The refined fits to the synchrotron and neutron powder patterns are shown in Figures 3a and 3b, respectively. The structure derived by simultaneous refinement of the synchrotron and neutron-diffraction data is shown in Figure 4. The atom coordinates and isotropic-displacement parameters are listed in Table 2; selected inter-atomic distances are presented in Table 3. A table of structure factors is available from the Depository Data, CISTI, National Research Council, Ottawa, Ontario K1A 0S2, Canada.

TABLE 1. SUMMARY OF CRYSTALLOGRAPHIC DATA, AND CONDITIONS OF COMBINED SYNCHROTRON X-RAY- AND NEUTRON-DIFFRACTION REFINEMENT OF THE STRUCTURE OF Ba₂[(UO₂)₂Ti₂O₈]

			X-ray	Neutron
space group	P2 ₁ /c	no. of profile parameters	15	11
<i>a</i> (Å)	6.4463(1)	no. of reflections	1293	582
<i>b</i> (Å)	8.5999(1)	no. of data points	1705	2454
<i>c</i> (Å)	10.2532(1)	background function	Chebyshev-1	
β (°)	75.936(1)	profile function	Pseudo-Voigt	Voigt
<i>V</i> (Å ³)	551.37(1)	μR	1.50	—
<i>Z</i>	4	λ (Å)	0.5001(1)	1.8845(1)
D _{calc} (g/cm ³)	6.253	R _B	0.032	0.039
T (K)	298	R _{wp}	0.090	0.063
no. of structural parameters	36	R _p	0.070	0.049
		χ ²	3.210	3.462

DESCRIPTION OF THE STRUCTURE

Ba₂[(UO₂)₂Ti₂O₈] has a carnotite-type crystal structure. Carnotite-type minerals are characterized by the uranyl divanadate structural motif, which is present in an extensive family including: K₂[(UO₂)₂V₂O₈] (Sundberg & Sillen 1949), A₂[(UO₂)₂V₂O₈] (A = Na, Tl and Rb) (Barton 1958), Cs₂[(UO₂)₂V₂O₈] (Appleman & Evans 1965, Tabuteau *et al.* 1985), Ag₂[(UO₂)₂V₂O₈] (Abraham *et al.* 1994), (NH₄)₂[(UO₂)₂V₂O₈](H₂O)₅ (Botto & Baran 1976), and Ba[(UO₂)₂V₂O₈] (Alekseev

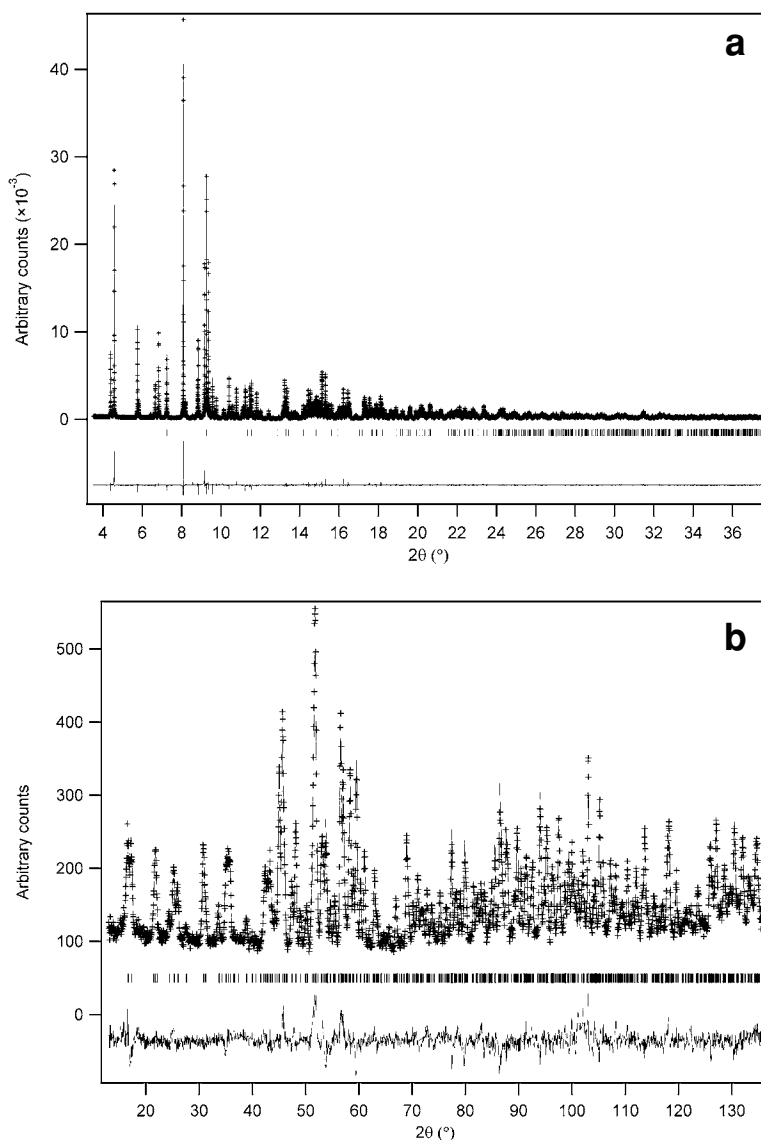


FIG. 3. Observed (+), calculated, and difference synchrotron X-ray (a), and neutron (b) powder-diffraction profiles for $\text{Ba}_2[(\text{UO}_2)_2\text{Ti}_2\text{O}_8]$ utilized in a multiple histogram Rietveld refinement.

et al. 2004). In each case, $[(\text{UO}_2)_2\text{V}_2\text{O}_8]$ sheets are formed by edge-sharing VO_5 square pyramids and UO_7 pentagonal bipyramids, with the alkali metal or alkaline earth (specifically Ba^{2+}) ions between the sheets. In addition to these vanadate compounds, $\text{Cs}_2[(\text{UO}_2)_2\text{Nb}_2\text{O}_8]$ (Gasperin 1987), $\text{Cs}_2[(\text{NpO}_2)_2\text{Mo}_2\text{O}_8]$ (Grigor'ev *et al.* 1995) and more recently $\text{A}[(\text{UO}_2)_2\text{Cr}_2\text{O}_8](\text{H}_2\text{O})_n$ ($\text{A} = \text{K}_2, \text{Rb}_2, \text{Cs}_2$ and Mg and $n = 0, 4$) (Locock *et al.* 2004)

have also been reported, each having the carnotite-type structure.

Other hydrated mineral forms have also been reported that display the $[(\text{UO}_2)_2(\text{V}_2\text{O}_8)]$ structural motif, including monoclinic sengierite $\text{Cu}_2(\text{UO}_2)_2\text{V}_2\text{O}_8(\text{OH})_2(\text{H}_2\text{O})_6$ (Piret *et al.* 1980), and the orthorhombic francevillite $(\text{Ba,Pb})[(\text{UO}_2)_2\text{V}_2\text{O}_8] \cdot 5\text{H}_2\text{O}$ (Mereiter 1986). Sengierite, in particular, shows a close structural relationship

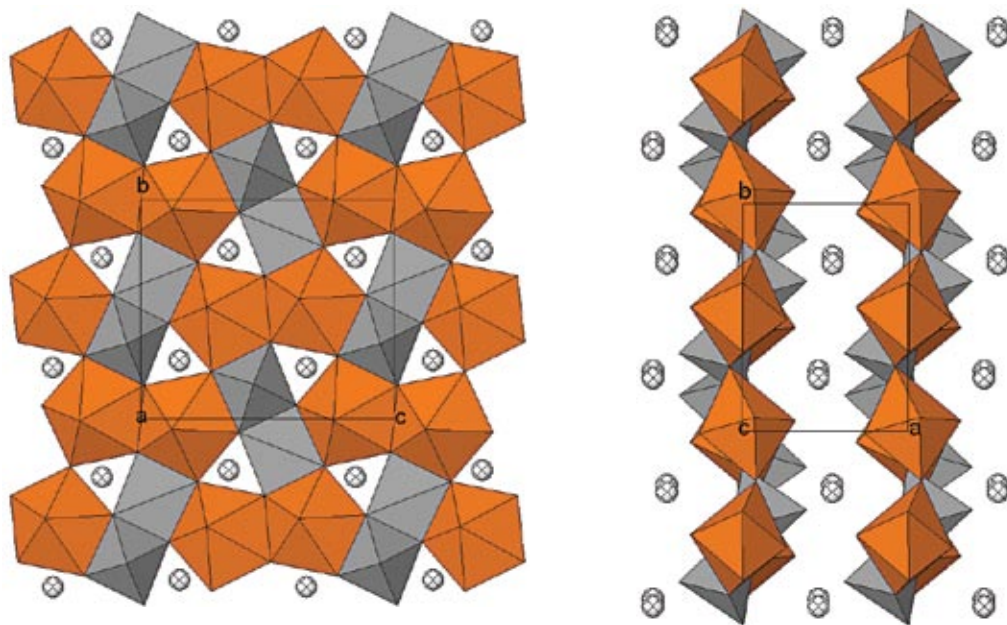


FIG. 4. Structure of Ba₂[(UO₂)₂Ti₂O₈] viewed along [100] (a), and along [001] (b). The UO₇ pentagonal bipyramids are shown in orange, TiO₅ square pyramids in grey, and the barium atoms are shown as hatched spheres.

TABLE 2. Ba₂[(UO₂)₂Ti₂O₈]: ATOM COORDINATES AND ISOTROPIC-DISPLACEMENT PARAMETERS

	<i>x</i>	<i>y</i>	<i>z</i>	<i>U</i> _{eq} (Å ²)
Ba	0.4579(2)	0.7661(1)	0.3471(1)	0.017(1)
U	0.0235(1)	0.9805(1)	0.1775(1)	0.002(1)
Ti	0.1104(4)	0.1506(3)	0.4506(2)	0.001(1)
O1	0.0796(7)	0.2144(5)	0.2776(5)	0.013(1)
O2	0.2612(7)	0.5099(5)	0.2607(4)	0.013(1)
O3	0.3130(7)	0.9534(5)	0.1240(4)	0.013(1)
O4	0.9298(7)	0.4382(5)	0.1108(4)	0.013(1)
O5	0.0041(8)	0.8477(5)	0.9873(5)	0.013(1)
O6	0.6195(7)	0.6582(5)	0.0563(5)	0.013(1)

TABLE 3. METAL-OXYGEN INTERATOMIC DISTANCES (Å) IN Ba₂[(UO₂)₂Ti₂O₈]

U –	O2	1.808(4)	Ba –	O6	2.683(6)
	O3	1.828(4)		O2	2.792(5)
	O5	2.284(5)		O2	2.815(4)
	O5	2.290(5)		O4	2.846(4)
	O4	2.292(5)		O1	2.978(4)
	O1	2.326(5)		O6	3.054(5)
Ti –	O1	2.396(4)	O5	3.088(4)	
	O6	1.727(6)	O3	3.117(5)	
	O5	1.896(5)	O3	3.121(5)	
	O1	1.913(6)	O3	3.348(4)	
	O4	1.925(4)	O6	3.516(5)	
	O4	1.970(5)			

with the vanadium-dominant carnotite phases, with essentially the same layer-structure but a substantially larger interlayer spacing, 10.085 Å.

The material reported here is the first reported structure of a uranyl titanate having the carnotite structure. It has the structural formula Ba₂[(UO₂)₂Ti₂O₈] and contains sheets of uranyl Ti⁴⁺ oxide with barium atoms located between the layers (Fig. 4b). Uranium is in 7-fold coordination by oxygen atoms in a pentagonal bipyramidal geometry. The axial uranyl (UO₂) bonds are relatively short, being 1.808(4) Å (U–O2) and 1.828(4) Å (U–O3) respectively. The remaining five U–O bonds range in length from 2.284(5) to 2.396(4) Å, averaging 2.317 Å in length. These bond distances are consistent

with those observed for other UO₇ polyhedra (Burns 1999) and carnotite-type materials (Appelman & Evans 1965, Tabuteau *et al.* 1985, Hughes *et al.* 2003, Alekseev *et al.* 2004). Titanium is present in an unusual 5-fold coordination, TiO₅, with square pyramid geometry. Two adjacent pyramids edge-share at their bases forming a Ti₂O₈ dimer with one pyramid apex above and one apex below the plane formed by the pyramid bases. In addition, two further edges of each TiO₅ square pyramid base are shared with those of UO₇ pentagonal bipyramids. Titanium forms four long Ti–O bonds in the basal plane of the pyramid, with lengths ranging from 1.896(4) to 1.970(5) Å, and one short apical bond at 1.727(6) Å (Ti–O6).

Five-fold coordinated Ti^{4+} is quite rare in oxide minerals. One of the few examples to show square pyramidal coordination of Ti is fresnoite, $\text{Ba}_2(\text{TiO})\text{Si}_2\text{O}_7$ (Moore & Louisnathan 1969), with a short apical Ti–O bond of 1.634 Å and four longer basal Ti–O bonds of 2.001 Å. Farges (1996) and Henderson *et al.* (2003) reported evidence for 5-fold titanium in Ti-silicate glasses using XANES and X-ray absorption spectroscopy. The latter authors observed a range of behaviors depending on the identity of other cations present. Homogeneous TiO_2 – SiO_2 glasses, as well as those containing alkaline-earth atoms, showed 5-fold Ti for low TiO_2 contents (~ a few wt%), through to mixtures of 4- and 5-fold coordination with increasing TiO_2 content. On the other hand, Na_2O -containing glasses showed a mixture of 4- and 5-fold coordination at low TiO_2 content, and pure 5-fold coordination at 14.3 wt% TiO_2 (Henderson *et al.* 2003).

Each Ba atom is coordinated in an irregular polyhedron consisting of nine nearest-neighbor oxygen atoms at distances ranging from 2.683(6) Å to 3.121(5) Å, and two longer contacts at 3.348(4) and 3.516(5) Å. Five of the “short” contacts lead to one $[(\text{UO}_2)_2\text{Ti}_2\text{O}_8]$ sheet, whereas the remaining six contacts complete the bridge to the adjacent sheet, in the direction of the *a* axis. For a given sheet, the orientation of these two “halves” of the Ba coordination sphere form distinct rows along the *c* axis, and these rows alternate along the *b* axis.

The structure of $\text{Ba}_2[(\text{UO}_2)_2\text{Ti}_2\text{O}_8]$ is essentially isostructural with compounds such as carnotite, $\text{K}_2(\text{UO}_2)(\text{VO}_4)\cdot 3\text{H}_2\text{O}$ and its Cs analogue; the variation in oxidation states between $\text{Ba}^{2+} + \text{Ti}^{4+}$ and $\text{K}^+ + \text{V}^{5+}$ allows each structure to remain electrostatically neutral with hexavalent uranium. In comparison, the presence of the divalent Ba in $\text{Ba}[(\text{UO}_2)_2\text{V}_2\text{O}_8]$ means that half of the potential interlayer $[(\text{UO}_2)_2\text{V}_2\text{O}_8]$ sites are vacant.

Bond-valence sums (BVS), listed in Table 4, were calculated using the refined metal–oxygen interatomic distances. R_0 and B parameters were taken from Brown & Altermatt (1985) for Ti^{4+} ($R_0 = 1.815$ Å, $B = 0.37$ Å) and Ba^{2+} ($R_0 = 2.285$ Å, $B = 0.37$ Å); these gave BVS of 4.24 and 1.75 valence units (*vu*), respectively. The BVS calculated for U^{6+} ($R_0 = 2.075$ Å, $B = 0.37$ Å) using parameters from Brown & Altermatt (1985) resulted in a larger-than-expected value of 6.62 *vu*. Recently,

Burns *et al.* (1997a) conducted an extensive study of the crystal chemistry of hexavalent uranium, examining the relationships between different coordination-geometries of uranyl and bond-valence parameters. They determined that for a pentagonal bipyramidal coordination of oxygen to hexavalent uranium, the parameters $R_0 = 2.051$ Å and $B = 0.519$ Å performed best for a broad range of well-refined structures. When used here, these parameters gave a much more reasonable value of 6.13 *vu*. Oxygen BVS were also calculated, returning values ranging from 1.77 (O6) to 2.25 *vu* (O2).

Bond-valence sums reported for other carnotite compounds, such as $\text{A}[(\text{UO}_2)_2\text{Cr}_2\text{O}_8](\text{H}_2\text{O})_n$ ($A = \text{K}_2, \text{Rb}_2, \text{Cs}_2; n = 0$ and $\text{Mg}; n = 4$) (Locock *et al.* 2004) give various bond-valence values for uranium, between 6.06 and 6.14 *vu* for the anhydrous K, Rb and Cs compounds, and 6.18 *vu* for the hydrated Mg compound. In each case, the parameters determined by Burns *et al.* (1997a) were used.

Although not explicitly reported in the structural studies of the uranyl vanadate compounds such as $\text{A}_2[(\text{UO}_2)_2(\text{V}_2\text{O}_8)]$ ($A = \text{Na}, \text{K},$ and Cs), the bond-valence sums of uranium can be calculated using the interatomic distances. The values are comparable to those reported here: $A = \text{Na}$ (6.20 *vu*), K (6.10 *vu*) (Abraham *et al.* 1993), as well as $A = \text{Cs}$ (6.14 *vu*) (Dickens *et al.* 1992). In contrast, a similar bond-valence calculation for U in $\text{Ag}_2[(\text{UO}_2)_2(\text{V}_2\text{O}_8)]$ (Abraham *et al.* 1994) gave a BVS of 5.61 *vu*. This is a reflection of the longer average axial (1.857 Å) and equatorial (2.384 Å) interatomic distances, compared to the alkali-metal-bearing carnotite-type phases. The phase $\text{Ba}[(\text{UO}_2)_2(\text{V}_2\text{O}_8)]$ (Alekseev *et al.* 2004) shows a larger-than-expected BVS, 6.51 *vu*. The BVS for Ba in this compound is low, at 1.54 *vu*, which may be a consequence of the highly irregular 11-fold coordination sphere, in combination with some disorder effects due to filling of only half of the interlayer space between the sheets.

Owing to the two-dimensional nature of these compounds, anhydrous vanadium-based carnotite-type phases $\text{A}_2[(\text{UO}_2)_2\text{V}_2\text{O}_8]$ ($A = \text{Ag}^+, \text{Na}^+, \text{K}^+, \text{Ti}^+, \text{Rb}^+$ or Cs^+) display a substantial variation in interlayer spacing, with *A*-site ionic radii (along the crystallographic axis *a*). The distance between *A*-site cations ranges from 5.895 Å for $\text{Ag}_2[(\text{UO}_2)_2\text{V}_2\text{O}_8]$ (Abraham *et al.* 1994) to 7.32 Å for $\text{Cs}_2[(\text{UO}_2)_2\text{V}_2\text{O}_8]$ (Appleman & Evans 1965), an increase of 24% (as a result of the ionic radii increasing from ~1.3 Å for Ag^+ to ~1.9 Å for Cs^+). By way of contrast, the other axes remain essentially constant, with the *b* and *c* axes increasing by only 1%. Given the same sheet-like nature of $\text{Ba}_2[(\text{UO}_2)_2\text{Ti}_2\text{O}_8]$, with an interlayer spacing of 6.446 Å and Ba^{2+} having an ionic radius of ~1.57 Å, one would also expect the formation of other titanate-based analogues with other large divalent cations. To date, no reports of the existence of other carnotite-like titanate phases have

TABLE 4. BOND-VALENCE (*vu*) CALCULATIONS FOR $\text{Ba}_2[(\text{UO}_2)_2\text{Ti}_2\text{O}_8]$

	U	Ba	Ti	Σ
O1	0.59, 0.51	0.15	0.77	2.02
O2	1.60	0.25, 0.24		2.09
O3	1.54	0.11, 0.10, 0.06		1.80
O4	0.63	0.22	0.74, 0.67	2.25
O5	0.64, 0.63	0.11	0.80	2.19
O6		0.34, 0.13, 0.04	1.27	1.77
Σ	6.13	1.75	4.24	

been made. It is noteworthy that given other carnotite-type vanadate (Tabuteau *et al.* 1985) and molybdate (Grigor'ev *et al.* 1995) compounds containing actinide elements such as Np, significant potential exists for the immobilization of high-level nuclear wastes in titanate-based materials of this structure type.

DISCUSSION

The chemical aspects associated with the long-term storage of spent nuclear fuel have received considerable attention over the past decade. Whereas UO_2 forms the basis of much spent nuclear fuel waste, U^{6+} minerals have been extensively studied, as they form alteration products on uraninite (UO_{2+x}) (Pearcy *et al.* 1994), or on spent fuel (Finn *et al.* 1998) under oxidizing conditions. Many of the structures that form as a result of the oxidation of UO_2 are based on U^{6+} polyhedra that form two-dimensional sheets incorporating cations of higher bond-valence within these sheets and monovalent cations, divalent cations, or H_2O as interlayer moieties. Our own study of $\text{Ba}_2[(\text{UO}_2)_2\text{Ti}_2\text{O}_8]$ demonstrates the potential of this compound to act as a nuclear waste-form and also display the aforementioned characteristics of infinite sheet formation and cation distribution. Leach rates for uranium in $\text{Ba}_2[(\text{UO}_2)_2\text{Ti}_2\text{O}_8]$ were found to be superior to other uranium titanate-based ceramics such as brannerite and Ca-U pyrochlore-group phases. Whether the oxidation state of uranium is a significant factor in waste-form durability is an issue of some debate; the role of crystal chemistry in the formation and stability of these compounds is clear, however. This study and that of Vance *et al.* (2002) have shown that the uranyl compound $\text{Ba}_2[(\text{UO}_2)_2\text{Ti}_2\text{O}_8]$ is formed with uranium present as U^{6+} , whether formed by sintering or by melting, and is also independent of whether air or argon was used. Typically, brannerite and pyrochlore waste-forms contain U^{4+} , although substitution at the uranium site by Ca^{2+} and trivalent rare-earth ions (James & Watson 2002, James *et al.* 2003) can lead to oxidation of uranium from U^{4+} to U^{5+} in ceramics produced in either air or argon. Studies by Burns and colleagues (1997b, 2004) have recently highlighted the importance of long-lived actinide elements incorporated into uranyl-bearing alteration phases produced from spent nuclear waste. Future studies are planned to examine the crystal chemistry and durability of analogues of $\text{Ba}_2[(\text{UO}_2)_2\text{Ti}_2\text{O}_8]$ containing other important actinide elements such as neptunium and plutonium.

ACKNOWLEDGEMENTS

We acknowledge the financial support of the Access to Major Research Facilities Program. We thank Drs. A.J. Locock, S.V. Krivovichev, and Associate Editor Uwe Kolitsch for their valuable comments.

REFERENCES

- ABRAHAM, F., DION, C. & SAADI, M. (1993): Carnotite analogues: synthesis, structure and properties of the $\text{Na}_{1-x}\text{K}_x\text{UO}_2\text{VO}_4$ solid solution ($0 \leq x \leq 1$). *J. Mater. Chem.* **3**, 459-463.
- ABRAHAM, F., DION, C., TANCRET, N. & SAADI, M. (1994): $\text{Ag}_2(\text{UO}_2)_2\text{V}_2\text{O}_8$: a new compound with the carnotite structure. Synthesis, structure and properties. *Adv. Mater. Res.* **1-2**, 511-520.
- ALEKSEEV, E.V., SULEIMANOV, E.V., CHUPRUNOV, E.V. & FUKIN, G.K. (2004): The crystal structure of $\text{Ba}(\text{VUO}_6)_2$. *Zh. Strukt. Khim.* **45**, 544-548.
- ALTOMARE, A., CASCARANO, G., GIACOVAZZO, C., GUAGLIARDI, A., BURLA, M.C., POLIDORI, G., & CAMALLI, M. (1994): SIRPOW.92 – a program for automatic solution of crystal structures by direct methods optimized for powder data. *J. Appl. Crystallogr.* **27**, 435-436.
- AMERICAN SOCIETY FOR TESTING AND MATERIALS (1997): *Standard Test Methods for Determining Chemical Durability of Nuclear, Hazardous, and Mixed Waste Glasses*. ASTM Designation: **C1285-97**.
- APPLEMAN, D.E. & EVANS, H.T., JR. (1965): The crystal structures of synthetic anhydrous carnotite, $\text{K}_2(\text{UO}_2)_2\text{V}_2\text{O}_8$, and its cesium analogue, $\text{Cs}_2(\text{UO}_2)_2\text{V}_2\text{O}_8$. *Am. Mineral.* **50**, 825-842.
- BARTON, P.B., JR. (1958): Synthesis and properties of carnotite and its alkali analogues. *Am. Mineral.* **43**, 799-817.
- BOTTO, I.L. & BARAN, E.J. (1976): On ammonium uranyl vanadate and the products of its thermal decomposition. *Z. Anorg. All. Chem.* **426**, 321-332.
- BROWN, I.D. & ALTERMATT, D. (1985): Bond-valence parameters obtained from a systematic analysis of the inorganic crystal structure database. *Acta Crystallogr.* **B41**, 244-247.
- BURNS, P.C. (1999): The crystal chemistry of uranium. In *Uranium: Mineralogy, Geochemistry and the Environment* (P.C. Burns & R. Finch, eds.). *Rev. Mineral.* **38**, 23-90.
- BURNS, P.C., DEELY, K.M. & SKANTHAKUMAR, S. (2004): Neptunium incorporation into uranyl compounds that form as alteration products of spent nuclear fuel: implications for geologic repository performance. *Radiochim. Acta* **92**, 151-160.
- BURNS, P.C., EWING R.C. & HAWTHORNE, F.C. (1997a): The crystal chemistry of hexavalent uranium: polyhedron geometries, bond-valence parameters, and polymerization of polyhedra. *Can. Mineral.* **35**, 1551-1570.
- BURNS, P.C., EWING R.C. & MILLER, M.L. (1997b): Incorporation mechanisms of actinide elements into the structures of U^{6+} phases formed during the oxidation of spent nuclear fuel. *J. Nucl. Mater.* **245**, 1-9.

- CARTER, M.L., VANCE, E.R., MITCHELL, D.R.G., HANNA, J.V., ZHANG, Z. & LOI, E. (2002): Fabrication, characterisation, and leach testing of hollandite, $(\text{Ba,Cs})(\text{Al,Ti})_2\text{Ti}_6\text{O}_{16}$. *J. Mater. Res.* **17**, 2578-2589.
- DICKENS, P.G., STUTTARD, G.P., BALL, R.G.J., POWELL, A.V., HULL, S. & PATAT, S. (1992): Powder neutron diffraction study of the mixed uranium–vanadium oxides $\text{Cs}_2(\text{UO}_2)_2(\text{V}_2\text{O}_8)$ and UVO_5 . *J. Mater. Chem.* **2**, 161-166.
- DICKSON, F.J., HAWKINS, K.D. & WHITE, T.J. (1989): Calcium uranium titanate – a new pyrochlore. *J. Solid State Chem.* **82**, 146-150.
- EBBINGHAUS, B.B., VAN KONYNENBURG, R.A., RYERSON, F.J., VANCE, E.R., STEWART, M.W.A., JOSTSONS, A., ALLENDER, J.S., RANKIN, T. & CONGDON, J. (1998): Ceramic formulation for the immobilization of plutonium. In *Waste Management '98* (Tucson) (CD-ROM: sess65/65-04).
- FARGES, F. (1996): Coordination of Ti in crystalline and glassy fresnoites: a high resolution XANES spectroscopy study at the Ti–K-edge. *J. Non-Cryst. Solids* **204**, 53-64.
- FINN, P.A., FINCH, R., BUCK, E. & BATES, J. (1998): Corrosion mechanisms of spent fuel under oxidizing conditions. *Mat. Res. Soc., Symp. Proc.* **506**, 123-131.
- GASPERIN, M. (1987): Synthèse et structure du niobouranate de césium. *Acta Crystallogr.* **C43**, 404-406.
- GRIGOR'EV, M.S., BATURIN, N.A., PLOTNIKOVA, T.E., FEDOSEEV, A.M. & BUDANTSEVA, N.A. (1995): Crystal structure of the complex neptunium(V) molybdate $\text{Cs}_2(\text{NpO}_2)\text{Mo}_2\text{O}_8$. *Radiochemistry* **37**, 15-18.
- HART, K.P., LUMPKIN, G.R., ZHANG, Y., LOI, E. & LEUNG, S. (1999): Durability and natural mineral studies carried out to support development of waste forms for immobilisation of plutonium. *Australian Nuclear Science and Technology Organisation Rep.* **R99m029**.
- HENDERSON, G.S., LIU XIAOYANG & FLEET, M.E. (2003): Titanium coordination in silicate glasses investigated using O K-edge X-ray absorption spectroscopy. *Mineral. Mag.* **67**, 597-607.
- HUGHES, K.-A., BURNS, P.C. & KOLITSCH, U. (2003): The crystal structure and crystal chemistry of uranosphaerite, $\text{Bi}(\text{UO}_2)_2\text{O}_2\text{OH}$. *Can. Mineral.* **41**, 677-685.
- HUNTER, B.A. (1998): Rietica – a visual Rietveld program. *Commission for Powder Diffraction Newsletter* **20**.
- JAMES, M., CARTER, M.L. & WATSON, J.N. (2003): The synthesis, crystal chemistry and structures of Y-doped brannerite $(\text{U}_{1-x}\text{Y}_x\text{Ti}_2\text{O}_6)$ and thorite $(\text{Th}_{1-x}\text{Y}_x\text{Ti}_2\text{O}_{6-\delta})$ phases. *J. Solid State Chem.* **174**, 329-333.
- JAMES, M. & WATSON, J.N. (2002): The synthesis and crystal structure of doped uranium brannerite phases $\text{U}_{1-x}\text{M}_x\text{Ti}_2\text{O}_6$ ($\text{M} = \text{Ca}^{2+}$, La^{3+} and Gd^{3+}). *J. Solid State Chem.* **165**, 261-265.
- LOCOCK, A.J., SKANTHAKUMAR, S., BURNS, P.C. & SODERHOLM, L. (2004): Syntheses, structures, magnetic properties, and X-ray absorption spectra of carnotite-type uranyl chromium(V) oxides: $\text{A}[(\text{UO}_2)_2\text{Cr}_2\text{O}_8](\text{H}_2\text{O})_n$ ($\text{A} = \text{K}_2$, Rb_2 , Cs_2 , Mg ; $n = 0, 4$). *Chem. Mater.* **16**, 1384-1390.
- MCCARTHY, G.J. (1977): High-level waste ceramics – materials considerations, process simulation, and product characterization. *Nucl. Technol.* **32**, 92-105.
- MEREITER, K. (1986): Crystal structure refinements of two francevillites, $(\text{Ba,Pb})[(\text{UO}_2)_2\text{V}_2\text{O}_8]\cdot 5\text{H}_2\text{O}$. *Neues Jahrb. Mineral., Monatsh.*, 552-560.
- MOORE, P.B. & LOUISNATHAN, S.J. (1969): The crystal structure of fresnoite, $\text{Ba}_2(\text{TiO})\text{Si}_2\text{O}_7$. *Z. Kristallogr.* **130**, 438-448.
- PEARCY, E.C., PRIKRYL, J.D., MURPHY, W.M. & LESLIE, B.W. (1994): Alteration of uraninite from the Nopal I deposit, Pena Blanca District, Chihuahua, Mexico, compared to degradation of spent nuclear fuel in the proposed U.S. high-level nuclear waste repository at Yucca Mountain, Nevada. *Appl. Geochem.* **9**, 713-732.
- PIRET, P., DECLERCQ, J.P. & WAUTERS-STOOP, D. (1980): Structure cristalline de la sengierite. *Bull. Minéral.* **103**, 176-178.
- RIETVELD, H.M. (1969): A profile refinement method for nuclear and magnetic structures. *J. Appl. Crystallogr.* **2**, 65-71.
- RINGWOOD, A.E., KESSON, S.E., REEVE, K.D., LEVINS, D.M. & RAMM, E.J. (1988): Synroc. In *Radioactive Waste Forms for the Future* (W. Lutze & R.C. Ewing, eds.). North-Holland, New York, N.Y. (233-334).
- RINGWOOD, A.E., KESSON, E.S., WARE, N.G., HIBBERSON, W. & MAJOR, A. (1979): Geological immobilisation of nuclear reactor wastes. *Nature* **278**, 219-223.
- SEARS, V.F. (1992): Neutron scattering lengths and cross sections. *Neutron News* **3**, 26-37.
- STEFANOVSKY, S.V., YUDINTSEV, S.V., NIKONOV, B.S., LAPINA, M.I. & ALOY, A.S. (2001): Effects of synthesis conditions on the phase composition of pyrochlore–brannerite ceramics. *Mat. Res. Soc., Symp. Proc.* **663**, 235-339.
- SUNDBERG, I. & SILLEN, L.G. (1949): On the crystal structure of KUO_2VO_4 (synthetic anhydrous carnotite). *Ark. Kemi* **1**, 337-351.
- SZYMAŃSKI, J.T. & SCOTT, J.D. (1982): A crystal structure refinement of synthetic brannerite UTi_2O_6 and its bearing on the rate of alkaline-carbonate leaching of brannerite in ore. *Can. Mineral.* **20**, 271-280.
- TABUTEAU, A., YANG, H. X., JOVE, J., THEVENIN, T. & PAGES, M. (1985): Cristallographie et étude par résonance Mössbauer de ^{237}Np de phases $\text{A}(\text{AnO}_2)(\text{V}_2\text{O}_8)$ ($\text{A} = \text{K}$, Rb , Tl ; $\text{An} = \text{U}$, Np) de structure carnotite. *Mat. Res. Bull.* **20**, 595-600.

- VANCE, E.R., CARTER, M.L., STEWART, M.W.A., DAY, R.A., BEGG, B.D. & BALL, C.J. (2002): Ionic size limits for A ions in brannerite (ATi_2O_6) and pyrochlore ($CaATi_2O_7$) titanate structures (A = tetravalent rare earths and actinides). In *Scientific Basis for Nuclear Waste Management XXV* (B.P. McGrail & C.A. Cragolino, eds.). Materials Research Society, Pittsburgh, Pennsylvania.
- VANCE, E.R., STEWART, M.W.A., DAY, R.A., HART, K.P., HAMBLEY, M.J. & BROWNSCOMBE, A. (1997): Pyrochlore-rich titanate ceramics for incorporation of plutonium, uranium and process chemicals. *Australian Nuclear Science and Technology Organisation Rep.* **R97m030**.
- VISSE, J.W. (1969): Fully automatic program for finding the unit cell from powder data. *J. Appl. Crystallogr.* **2**, 89-95.
- ZHANG, Y., HART, K.P., THOMAS, B.S., ALY, Z., LI, H. & CARTER, M. (2001): Dissolution of synthetic brannerite at 90°C. *Mat. Res. Soc., Symp. Proc.* **663**, 341-345.

Received February 15, 2005, revised manuscript accepted October 15, 2005.